1-1-2019

Computational fluid dynamics-based modeling of liquefied soils

S. Banerjee
University of Vermont

J. Chen
University of Illinois Urbana-Champaign

D. L. Hitt
University of Vermont

M. M. Dewoolkar
University of Vermont

S. M. Olson
University of Illinois Urbana-Champaign

Recommended Citation

Computational fluid dynamics-based modeling of liquefied soils

S. Banerjee
Graduate student, University of Vermont, Burlington, VT, USA, sbanerj1@uvm.edu

J. Chen
Graduate student, University of Illinois, Urbana-Champaign, IL, USA, jchen259@illinois.edu

D. L. Hitt
Professor, Mechanical Engineering, University of Vermont, Burlington, VT, USA, Darren.Hitt@uvm.edu

M. M. Dewoolkar
Professor, Civil and Env. Eng., University of Vermont, VT, USA, Mandar.Dewoolkar@uvm.edu

S. M. Olson
Associate Professor, University of Illinois, Urbana-Champaign, IL, USA, olsons@illinois.edu

ABSTRACT: The residual shear strength of liquefied soil is a key parameter in evaluating liquefaction flow failures. Results from a series of dynamic centrifuge experiments where the shear strength of liquefied soil was inferred by measuring the force required to pull a thin metal plate (coupon) horizontally through the liquefied soil are assessed here using a computational fluid dynamics (CFD) based model. Viscosity is a key parameter for the Newtonian fluid constitutive model used in the simulations, and apparent viscosities of liquefied soil in the range of about 5,800 – 13,300 Pa·s were obtained when the CFD model was calibrated against coupons pulled through liquefied soil in dynamic centrifuge tests. These computational values agree reasonably with apparent viscosities of liquefied soil reported in the literature when the Reynold's numbers exceeded 1.0. Importantly, the CFD simulations illustrated that in cases where Reynold's numbers are < 1.0, apparent viscosities of liquefied soil back-calculated using simplistic closed-form solutions commonly applied in geotechnical literature are several orders of magnitude too large; and therefore, such closed-form solutions should not be used for these cases.

1 INTRODUCTION

Countless hydraulic fill dams, tailings dams, levees, and other natural and manmade slopes and other earth structures contain or are founded on loose, saturated granular soils, rendering them vulnerable to liquefaction flow failures during earthquakes. Although flow failures are uncommon, the potentially catastrophic consequences of these failures dramatically elevate the associated risk. Analytically modeling soil behavior during flow failures, especially in numerical schemes, is not a straightforward task. Because saturated, contractive soils undergo significant softening and large strains during liquefaction and flow, currently available soil mechanics-based constitutive models are unable to reliably capture this behavior. Therefore, new approaches are needed. This paper explores applying computational fluid dynamics (CFD) analysis for modeling the behavior of liquefied soils. An important parameter for modeling liquefied soil as a fluid is its apparent viscosity. Towhata et al. (1999) estimated the apparent viscosity of liquefied sand by measuring the drag force on a cylindrical pipe while pulling it through liquefied sand in 1g tests. Similarly, de Alba and Ballestero (2005, 2006) measured the drag forces on a sphere and a thin plate falling through liquefied sand in modified triaxial specimens to infer the apparent viscosity of liquefied soils. Dewoolkar et al. (2015) inferred the shear strength of liquefied sand by measuring the drag forces on a thin plate (coupon) pulled through the liquefied sand in flight in a centrifuge model.

In this study, the authors analyzed the Dewoolkar et al. (2015) coupon-pull centrifuge experiments using CFD, modeling the liquefied soil as a Newtonian fluid. Further, the authors calculated the apparent viscosities of liquefied sand from the CFD results and compared the same back-calculated from experiments reported in the literature.

2 LITERATURE REVIEW

A rheological approach has been employed by numerous researchers to quantify the residual strength of liquefied soils interpreted from small-scale 1g and centrifuge physical models as well as triaxial tests. In many of these tests, embedded objects (e.g., sphere, flat plate, and cylinder) were pulled through the soil after inducing liquefaction. Common considerations were that liquefaction should be maintained during the movement of the object and the object should move far enough to mobilize large strains in the liquefied soil.

Towhata et al. (1999) measured drag force on an embedded cylinder pulled laterally through a 1g model of saturated sand that was liquefied by shaking. Free-field pore pressure transducers located in the model soil confirmed that the soil remained liquefied during the movement of the cylinder. This study showed that the drag force measured while the excess pore pressure remained high increased with the velocity of cylinder movement. Given the low Reynolds number (Re) of the flow, Towhata et al. (1999) used the following equation based on the Stokes's drag law to estimate the apparent viscosity of the liquefied soil:

$$D_{\text{cylinder}} = \frac{4\pi\mu VL}{2.002 - \ln(\rho Vd / \mu)} \tag{1}$$

where D_{cylinder} = drag force, μ = apparent viscosity, V = cylinder velocity, L = cylinder length, ρ = soil density, and d = cylinder diameter. Equation 1 yielded apparent viscosities of 100 to 2,600 Pa·s for the liquefied sand. Towhata et al. (1999) also reported apparent viscosities inferred from other similar studies, which are summarized in Table 1.

Hwang et al. (2006) measured drag forces on a sphere sinking in liquefied soil and by pulling a cylinder through liquefied soil. Initial relative densities of the soils ranged from 34 to 64%. Liquefaction was induced by impact and upward seepage, respectively. To estimate apparent viscosity, Hwang et al. (2006) used Equation (1) for the cylinder test and the following equation based on Stokes's drag law for the sphere tests (White 1979):

$$D_{\text{sphere}} = 3\pi\mu dV \tag{2}$$

where d = sphere diameter, V = sphere velocity. The apparent viscosities ranged from 6,340 to 11,610 Pa·s in the sphere tests and 1,100 to 5,000 Pa·s in the cylinder tests are significantly larger than those estimated by Towhata et al. (1999). In addition, the apparent viscosities at different pulling speeds of the cylinder showed a shear thinning behavior, i.e., apparent viscosity decreased with increasing pulling speed. As a result, Hwang et al. (2006) concluded that liquefied soil behaves like non-Newtonian fluid.

de Alba and Ballestero (2005, 2006) recognized some of the limitations of small-scale 1g model tests (unrealistically low stress levels and difficulty in maintaining undrained conditions) and experimented with a 1.27 cm diameter sphere and a 2.54 cm x 2.54 cm x 0.16 cm flat plate (coupon) displacing axially, pulled by a deadweight, through triaxial specimens (7.1 cm in diameter and 24 cm in height) of saturated sand, after inducing liquefaction by cyclic loading. These tests were conducted under equal all-around consolidation stresses of 70 and 140 kPa – significantly greater than those in small-scale 1g physical models. Undrained conditions were maintained during their tests. Test results indicated that liquefied soils exhibit a viscous behavior where the drag force on the sphere or coupon increased and the apparent viscosity decreased as the velocity increased, and similar to Hwang et al. (2006), they concluded that liquefied soil may be regarded as a non-Newtonian fluid. Considering the Reynolds number mobilized during their tests, de Alba and Ballestero (2005) recommended the use of a coupon instead of a sphere so that the flow remained laminar over a much larger range of velocities.

Interestingly, de Alba and Ballestero (2005, 2006) observed that the drag force stabilized once the object reached a velocity around 50 cm/s. Apparent viscosities calculated in that stabilized range are typically within 30 – 1,500 Pa·s, obtained by Equations (2) and the following equation for a plate (Schlichting 1979):

$$D_{\text{coupon}} = 1.328 BL^{1/2} V^{3/2} \mu^{1/2} \rho^{1/2} \tag{3}$$

where B = coupon width, L = coupon length and V = coupon velocity.

Table 1 summarizes apparent viscosities of liquefied soils back-calculated from various sources including the experiments described above. One estimate is based on the subsidence of Niigata Airport Building in 1964 (Towhata and Horikoshi 1997) while others are based on modified triaxi-

Table 1 Summary of apparent viscosities of liquefied soils estimated from 1g physical model tests, triaxial tests and case studies reported in the literature

Reference	Test type	Method of liquefaction	Velocity	Dr	Apparent Viscosity
			(cm/s)	(%)	(Pa·s)
de Alba and Ballestero (2005)	Triaxial cell, pulling coupon	Cyclic loading	up to 160	(-30)-30	40-1,500
de Alba and Ballestero (2006)	Triaxial cell, pulling sphere	Cyclic loading	up to 110	30	30-140
Towhata et al. (1999)	1-g, pulling cylinder	Shaking	0.3-1.9	(-20)-30	510-2,600
	1-g, pulling cylinder			(-30)-(-20)	130-660
Hwang et al. (2006)	1-g, sinking sphere	Impact	2.5-5	34-64	6,340-11,610
	1-g, pulling cylinder	Upward seepage	2.03-8.61	34	1100-5,000
The following data reported by Towhata et al. (1999) are iterated here:					
Miyajima et al. (1994a)	1-g, sinking sphere	Shaking	-	-	70-400
Miyajima et al. (1994b)	1-g, pulling sphere	Boiling	-	-	
Miyajima et al. (1995)	1-g, sinking sphere	Shaking	1-5.2	-	108
Ohtomo et al. (1993)	1-g, pulling sphere	Boiling	-	50	1000
Sato et al. (1994a)	1-g, pulling sphere	Shaking	1-6	10-50	up to 5,000
	1-g, pulling cylinder	Shaking	1-5	25-45	up to 8,000
Sato et al. (1994b)	50-g, flow of slope	Shaking	-	25-30	2,800-4,000
Sasaki et al. (1997)	1-g, subsidence of foundation	Shaking	-	28-44	110-230
Towhata and Horikoshi (1997)	Subsidence of prototype building foundation	1964 Niigata earthquake	-	-	2.5-500
Takada and Nagai (1987)	1-g, sinking sphere	Shaking	-	-	500-8,000
Yuasa et al. (1994)	1-g, pulling sphere during shaking	Shaking	-	35-60	2-14
	1-g, pulling sphere after shaking	Shaking	-	30-50	16-20
	1-g, viscometer	Boiling	-	20-50	0.25-40
Toyota (1995)	1-g, flow of slope	Impact	-	(-20)-7	100-200
The following were reported by Hwang et al. (2006) and Towhata et al. (1999):					
Hamada and O'Roorke (1992)	1-g, pulling sphere	Unknown	-	34	300-5,000
Hamada et al. (1993)	1-g, pulling cylinder, pile, sphere	Unknown	-	-	up to 8,000
Kawakami et al. (1994)	1-g, sphere	Shaking	0.25-1.5	27-51	14.7-30.4
	1-g, viscometer	Upward seepage	1.5-4.5 rpm	20-50	0.24-39
	Large ground displacement experiment	Shaking	-	-	147-981
Towhata et al. (1992)	Flow of slope	-	-	38	900
Vargas and Towhata (1995)	1-g, pulling cylinder	Shaking	up to 1.9	(-30)-30	90-1,510
Zhang et al. (1994)	Undrained triaxial test	Cyclic loading	10-60%/s	-	3,600-8,900

-al tests (de Alba and Ballestero 2005, 2006) and 1g physical model tests (Towhata et al. 1999, Hwang et al. 2006). As expected, the back-calculated apparent viscosities reported in Table 1 show significant scatter. This scatter can be attributed to uncertainties involved in case history analysis, variations in effective stress, drainage conditions, sand relative density, deviation from closed-form solutions (i.e., turbulent flow), and variable strain rates, among other variations.

   Figure 1 presents the apparent viscosities summarized in Table 1 with respect to relative density. Despite the scatter, most of the back-calculated apparent viscosities fall within a wide range of about 30 to 3000 Pa·s. In comparison, the viscosity of water at 20°C is 0.001 Pa·s. Therefore, the apparent viscosity of liquefied soil may be 4 to 6 orders of magnitude larger than that of water.
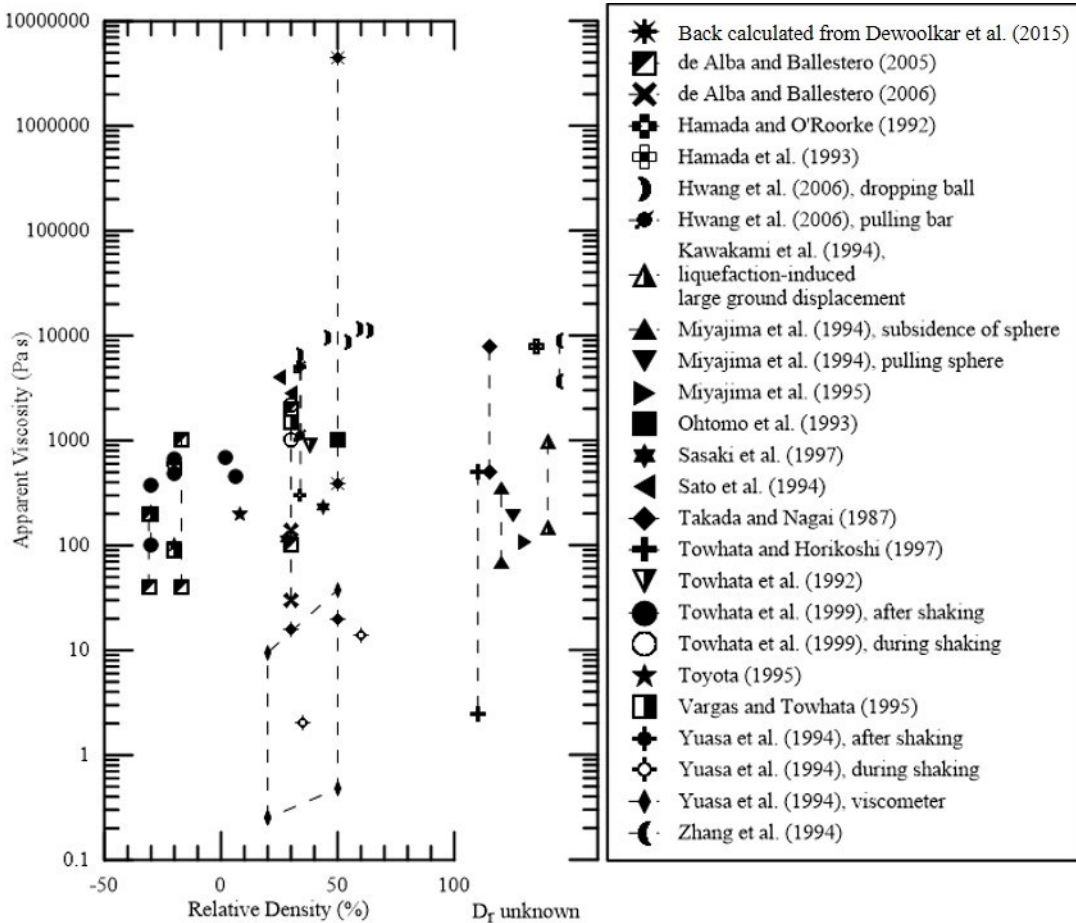

Figure 1. Apparent viscosities of liquefied sand back-calculated from modified triaxial tests, 1g physical model tests, dynamic centrifuge tests, and field case histories.

3   AVAILABLE DYNAMIC CENTRIFUGE TEST RESULTS

Inspired by the de Alba and Ballestero (2005, 2006) experiments, Dewoolkar et al. (2015) pulled a coupon (76.2 mm long, 25.4 mm wide, and 2.25 mm thick) horizontally through a saturated sand model in dynamic centrifuge models using a motor assembly mounted on top of the model container (121.9 cm length x 30.5 cm width x 43.5 cm height). Six coupon-pull experiments were successful. These experiments were done at two different g levels; 25g and 50g, and the coupon was pulled at three different speeds 5 cm/s, 30 cm/s and 60 cm/s. The increased g-level and the use of viscous methylcellulose as the pore fluid resulted in more realistic effective stresses and maintained high excess pore pressures longer after the shaking ceased. The coupon pulling (drag) force was measured using a torque transducer integrated with the motor assembly. The measured force increased as the coupon pull was initiated. As the centrifuge model was shaken, excess pore pressure increased and the measured pulling force dropped rapidly and stabilized at a minimum

value after the shaking ceased. Dewoolkar et al. (2015) used the minimum pulling force mobilized after liquefaction to infer the residual shear strength of the liquefied sand.

The apparent viscosities of the liquefied sands in the centrifuge tests of Dewoolkar et al. (2015) are estimated here using Equation (3), with measured drag forces reduced to exclude forces on the leading edge and transverse surfaces of the coupon. Computed apparent viscosities ranged from around 400 Pa·s for high coupon velocity (30 and 60 cm/s) to over 10^6 Pa·s for low coupon velocity (5 cm/s). The apparent viscosity for low coupon velocity is quite large; however, de Alba and Ballestero (2005) suggested that back-calculated apparent viscosity can be on the order of 10^6 Pa·s for small strain rates, which is consistent with the low coupon pull velocity tests from Dewoolkar et al. (2015).

4 COMPUTATIONAL FLUID DYNAMICS MODEL

A numerical model of the Dewoolkar et al. (2015) experiments was developed using CFD techniques. For simplicity, a 2-D model was assumed that represents plain strain conditions; clearly this assumption deviates from the finite aspect ratio of an actual coupon and does not incorporate any edge effects associated with a finite width. We posit that the side wall shear force contribution is likely to be a fraction of the overall force acting on the coupon. This hypothesis is based on the fact that the side areas represent < 9% of the total surface area of the coupon. Assuming the shear stresses on the sides are of similar order of magnitude as the top/bottom surfaces, it follows their contribution to the total force will be relatively minor.

For the CFD model, an Eulerian reference frame was chosen that moves with the coupon so that the coupon appears stationary and the liquefied soil flows over the coupon; this is dynamically equivalent to a moving coupon in a quiescent fluid. Transient effects of the coupon start-up acceleration were not considered and a steady-state condition was assumed.

For low Reynolds number associated with this study [Re < 1], a steady incompressible laminar flow state exists with the flow governed by the Navier-Stokes equations:

$$\boldsymbol{\nabla}.\boldsymbol{u} = 0 \qquad\qquad\qquad\qquad\qquad (4)$$

$$\rho(\boldsymbol{u}.\boldsymbol{\nabla})\boldsymbol{u} = -\boldsymbol{\nabla}p + \mu\nabla^2\boldsymbol{u} \qquad\qquad\qquad\qquad (5)$$

where **u** = velocity, p = pressure, ρ = soil density and μ = soil dynamic viscosity. Note that hydrostatic pressure effects are negligible over the vertical scale of the coupon and so do not appear in the governing equations.

In this study, a Newtonian constitutive model was assumed wherein the shear stress (τ) is linearly related to the strain rate ($\dot{\gamma}$) with a constant slope equal to the dynamic viscosity, μ. It is recognized that a non-Newtonian behavior for a liquefied soil has been suggested (de Alba and Ballestero 2005 and 2006, Towhata et al. 1999, Hwang et al. 2006), however a Newtonian model was considered acceptable here for this exploratory attempt of CFD simulations, which is expected to provide a reasonable estimate of apparent viscosity of liquefied soils.

A computational domain was created that effectively modeled the flow past the coupon as one existing in an infinite domain without solid boundaries. This assumption is justified given the size of the centrifuge container compared to the coupon size. The symmetry of the problem further allows us to model only the flow over the top (or bottom) of the coupon (plane-strain conditions). The inlet boundary condition is that of uniform velocity equal to the coupon velocity whereas the outlet condition is that of constant pressure. The coupon surface is a no-slip wall condition owing to the viscous flow. Lastly, a constant velocity was imposed on the upper boundary equal to and parallel with the inlet velocity; this treats the upper boundary as being an "infinite" distance away from the coupon so that flow is unperturbed. The required domain height was determined via numerical experiments to verify that this imposed condition is consistent with the calculated flow field. In a similar manner, the required extents of the domain upstream and downstream of the coupon were also determined.

The domain was constructed so as to leverage the top-bottom symmetry of the flow about the coupon. Referring to Figure 2, a computational domain of size 726.2 mm x 1001.5 mm satisfied these constraints in which 400 mm is the upstream length, 250 mm is the downstream length and

the upper boundary is 1000 mm above the coupon. The need for the significant upper extent of the domain is a consequence of the low Reynolds number of the flow. The domain was meshed with quadrilateral elements concentrated near the coupon surface (see Figure 2) to accurately resolve the viscous boundary layer. Grid sensitivity studies were performed and a final mesh was identified that was sufficiently insensitive to further refinement; the final mesh consisted of 403,450 elements.
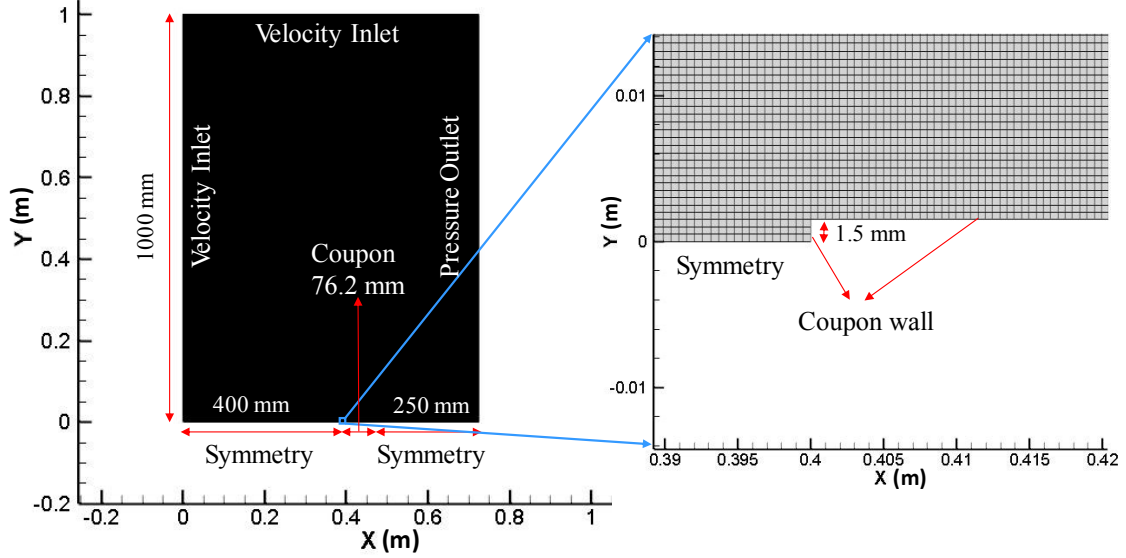

Figure 2. Computational domain mesh and mesh elements near the coupon.

The Navier-Stokes equations were solved using a finite-volume-based CFD code (ANSYS Fluent). A second-order upwinding scheme was used to discretize the convective derivative and the SIMPLE algorithm was used for pressure-velocity coupling. Convergence of the iterated solution was determined by monitoring both global residuals (e.g., continuity) as well as point monitors located at key points along the coupon surface.

5 COMPARISON BETWEEN COMPUTATIONAL RESULTS AND CLOSED-FORM SOLUTIONS

In an effort to validate the computational model, wall shear stress distributions along the coupon surface were compared to the closed-form Blasius boundary layer solution for laminar flow over an infinite flat plate (Blasius, 1908). Specifically, the wall shear stress distribution is given by (Schlichting, 1979):

$$\tau_w\left(x\right) = 0.332\sqrt{\frac{\rho\mu V^3}{x}} \tag{6}$$

where $\tau_w(x)$ = wall shear at a distance x from the leading edge of the flat plate; V = free-field stream velocity, i.e. velocity outside of the boundary layer.

An interesting observation was made while comparing the wall shear stress distributions from CFD simulations with the Blasius solution, as shown in Figure 3. Here, the simulated wall shear values closely matched the Blasius wall shear values when viscosity is very low, ranging from 0.001 Pa·s (water) to 0.1 Pa·s. However, as viscosity increases to a range between 100 – 1,500 Pa·s, the Blasius solution yielded wall shear values many orders of magnitude smaller than the simulated wall shear values. This difference between the closed-form Blasius solution and the simulation results at higher viscosities is a result of small Reynolds numbers of the flow. According to White (1979), at small Reynolds numbers (< 1.0), the viscous region around a flat plate is broad and extends far upstream of the plate, developing a boundary layer very different than that assumed by Blasius (1908). As mentioned earlier, de Alba and Ballestero (2005) back-

calculated very high apparent viscosities of liquefied sand (> 10^6 Pa·s) at low velocities, and hence, small Reynolds numbers using the closed-form solution. Similarly, centrifuge tests of Dewoolkar et al. (2015) at coupon pulling speed of 5 cm/s yielded high apparent viscosities when the closed-form solution was used. These results illustrate that Blasius solution should not be used to estimate apparent viscosities of liquefied soil at small Reynolds numbers (< 1.0). In those cases, numerical simulations are a much better approach.

Dewoolkar et al. (2015) reported the residual shear strengths to be 7.8 – 17.9 kPa for coupon pulling speed of 5 cm/s. CFD simulations gave coupon wall shear values between 0.134 and 13.44 kPa for 5 cm/s flow velocity and 100 – 10,000 Pa·s viscosity. Clearly, the computed wall shear has a linear relationship with viscosity, consistent with the Newtonian fluid properties. Therefore, the apparent viscosity of liquefied sand is extrapolated linearly to values of 5,798 – 13,309 Pa·s for the measured residual shear strengths of 7.8 – 17.9 kPa. The resulting liquefied sand viscosities agree reasonably well with the literature.
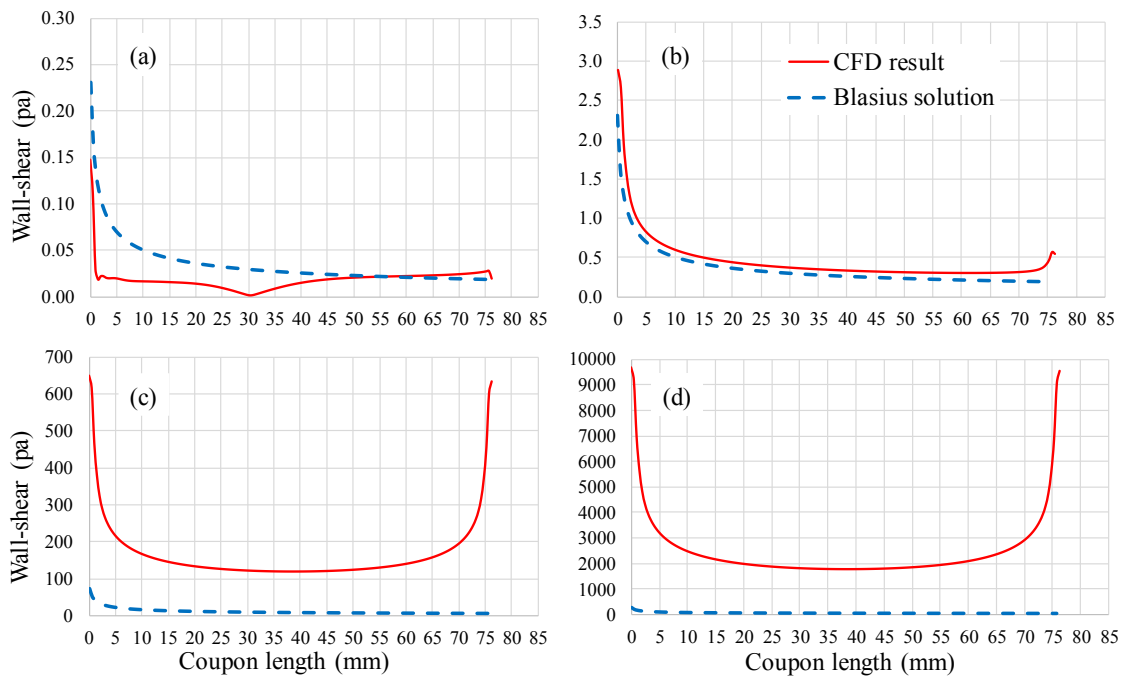

Figure 3. Comparison of wall shear over a flat plate computed by CFD simulations and closed-form Blasius (1908) solution using a coupon speed of 5 cm/s and varying μ from 0.001 Pa·s (water) to 1500 Pa·s. (a) μ = 0.001 Pa·s (water) and Re = 144.15; (b) μ = 0.1 Pa·s and Re = 1.4415; (c) μ = 100 Pa·s and Re = 1.4415×10^{-3}; and (d) μ = 1500 Pa·s and Re = 9.61×10^{-5}.

6 CONCLUSIONS

This study attempted to model liquefied soil as a fluid using CFD; assessed the liquefied soil's apparent viscosities reported in the literature; and evaluated these viscosities using the results of CFD simulations. A review of the literature revealed that apparent viscosities of liquefied soils largely have been inferred from small-scale 1g physical models as well as triaxial tests. The inferred apparent viscosities are scattered and cover a large range (<1 to >10^6 Pa·s) with most values falling between 30 and 3,000 Pa·s. CFD modeling considering Newtonian model indicated the viscosities of liquefied soils to be in the range of about 5,800 – 13,300 Pa·s. These values agree reasonably with values reported in the literature when Re > 1. Importantly, the CFD simulations illustrated that in cases with Re < 1, apparent viscosities back-calculated using closed-form solutions are many orders of magnitude larger than those inferred from the CFD simulations. Thus, closed-form solutions should not be used to infer apparent viscosity of liquefied soil for these cases.

REFERENCES

Blasius, H. 1908, Grenzschichtenin Flüssigkeiten mit kleiner Reibung, *Z. Math. Phys*. 56, 1.

de Alba, P. & Ballestero, T. 2005. Liquefied granular materials as non-Newtonian fluids: A laboratory study. *Proc., Geo-Frontiers,* ASCE, Reston, VA.

de Alba, P. & Ballestero, T. 2006. Residual strength after liquefaction: A rheological approach. *Soil Dyn. Earthquake Eng.,* 26(2-4), 143-151.

Dewoolkar, M. M., Hargy, J., Anderson, I., de Alba, P., & Olson, S. M. 2015. Residual and post liquefaction strength of a liquefiable sand, ASCE *Journal of Geotechnical and Geoenvironmental Engineering,* (IF 2.092), 142(2), 10.1061/(ASCE)GT.1943-5606.0001374, 04015068.

Hamada, M., O'Rourke, T D. 1992. Case studies of liquefaction and lifeline performance during past earthquakes. *Japanese Case Studies, Technical Report NCEER-92-0001*. Buffalo, NY: NCEER.

Hamada, M., Sato, H., Doi, M. 1993. An experimental study of mechanical properties of liquefied soil and large ground displacement. *US–Japan Workshop on Site Response and Ground Failures during Earthquakes,* Napa Valley, California.

Hwang, J. I., Kim, C. Y., Chung, C. K., & Kim, M. M. 2006. Viscous fluid characteristics of liquefied soils and behavior of piles subjected to flow of liquefied soils. *Soil Dyn. Earthquake Eng.,* 26(2–4), 313–323.

Kawakami, T., Suemasa, N., Hamada, M., Sato, H., Katada, T. 1994. Experimental study on mechanical properties of liquefied sand. *Proc. from the Fifth US-Japan Workshop on Earthquake Resistant Design of Lifeline Facilities and Countermeasures against Soil Liquefaction*, Salt Lake City, USA, Tech. report NCEER-94-0026:285–99.

Miyajima, M, Hasegawa, M, Kitaura, M, Koike, T, Kitano, Y. 1994a. Experimental study on effects of liquefaction-induced lateral spreading on buried structures. *Proc. Ninth Japan Earthquake Engineering Symposium*, 2:1363–1368 (in Japanese).

Miyajima, M., Kitaura, M., Kitano, Y. 1994b. Model tests on variation of soil properties with the extent of liquefaction. *Proc. Annual Conf. JSCE*, III:548–549 (in Japanese).

Miyajima, M., Kitaura, M., Koike, T., Hasegawa, M.1995. Experimental study on characteristics of liquefied ground flow. *Proc. of the ISTokyo'95*, *First International Conference on Earthquake Geotechnical Engineering*, Balkema, 969–974.

Ohtomo, K., Iwadate, T., Shimizu, M., Shumuta, Y., Hamada, M. 1993. Horizontal load exerted on pile foundation by lateral flow of liquefied sand. *Proc. 22nd Earthquake Engineering Conference of JSCE,* 95–98 (in Japanese).

Sasaki, Y., Udaka, K., Miyamoto, Y. 1997. Prediction of subsidence of embankment resting on liquefied subsoil with consideration on duration of high pore pressure. *Proc. Tech. Conf., Chugoku Chapter of JSCE*, (in Japanese).

Sato, H., Doi, M., Ohbo, N., Honda, M., Hamada, M. 1994b. Dynamic centrifugal tests on lateral flow of sandy ground. *Proc. 49th Annual Conference of JSCE*, 3A:520–521 (in Japanese).

Sato, H., Hamada, M., Doi, M. 1994a. An experimental study of effects of laterally flowing ground on in-ground structures. *Proc. Fifth Japan–US Workshop on Earthquake Resistant Design of Lifeline Facilities and Countermeasures against Soil Liquefaction*. Tech. Report NCEER-94-0026:405–414.

Schlichting, H., 1979, Boundary layer theory, *McGrew-Hill, Inc.,* ISBN 0-07-055334-3.

Takada, S., Nagai, J. 1987. Dynamic stiffness and damping in liquefied ground. *The Construction Engineering Research Institute Foundation*, Report 29:53–98 (in Japanese).

Towhata, I., Horikoshi, K. 1997. Analysis on subsidence of building resting on liquefied sandy ground. *Proc. 32nd Annual Convention of Japanese Geotechnical Society*, 1:973–974 (in Japanese).

Towhata, I., Sassaki, Y., Tokida, K., Matsumoto, H., Tamira, Y., Yamada, K. 1992. Prediction of permanent displacement of liquefied ground by means of minimum energy principle. *Soils Found* 32(3):97–116.

Towhata, I., Vargas-Monge, W., Orense, R. P., & Yao, M. 1999. Shaking table tests on subgrade reaction of pipe embedded in sandy liquefied subsoil. *Soil Dyn. Earthquake Eng.,* 18(5): 347-361.

Toyota, H. 1995. Shaking table tests and analytical prediction on lateral flow of liquefied ground. *Doctoral thesis, The University of Tokyo*, 380 (in Japanese).

Vargas, W., Towhata, I. 1995. Measurement of drag exerted by liquefied sand on buried pipe. *Proc. of the First International Conference on Earthquake Geotechnical Engineering*. 2:975–80.

White, F. M., 1979, Fluid mechanics. *McGrew-Hill, Inc*. ISBN 0-07-069667-5.

Yuasa, A., Sato, H., Doi, T., Kawakami, T., Hamada, M. 1994. An experimental study on fluid properties of liquefied sand. *Proc. Ninth Japan Earthquake Engng Symp*, 1:877–882 (in Japanese).

Zhang, J. M. 1994. Transient shear strength of saturated sand under cyclic loading considering strain-rate effect. *Soils Found* 4:51–65.